*Proceedings of the 3rd International Conference on Fluid Flow, Heat and Mass Transfer (FFHMT'16)*
*Ottawa, Canada – May 2 – 3, 2016*
*Paper No. 165*

# Numerical Study on Small-Scale Fire Whirl using Large Eddy Simulation

**A.C.Y. Yuen[1], G.H. Yeoh[1], R.K.K. Yuen[2], S.M. Lo[2]**
[1]School of Mechanical and Manufacturing Engineering, UNSW
Room 401, Ainsworth Building (J17), UNSW, Sydney, Australia
c.y.yuen@unsw.edu.au; g.yeoh@unsw.edu.au
[2]Department of Architecture and Civil Engineering, City University of Hong Kong
B6518, Blue Zone, Academic 1, City University of Hong Kong, Tat Chee Avenue, Hong Kong SAR
bckkyuen@cityu.edu.hk; bcsmli@cityu.edu.hk

***Abstract*** **-** Fire whirl is a rotating fire with either a fixed or revolving flame centre-core caused by unbalanced entrainment. In general, the flame height of a fire whirl is significantly larger than that of a free standing fire. It is suggested by several studies that fire whirl is a disastrous scenario especially in urban or bush fires since it can greatly promote the fire spread and escalate the thread to human lives and species. In this paper, as a preliminary study, the fire whirl behaviour has been studied numerically using the Fire Dynamics Simulator (FDS) ver 6.1.2 which is based on the large eddy simulation (LES). It incorporates the mixture fraction based combustion model along with soot formation, the subgrid-scale (SGS) turbulence model, radiation transfer equation (RTE) model which are fully coupled and interactive. This allows the modelling of all essential chemical and physical behaviours that occur during the fire whirling processes. A small-scale vertical shaft with a base of 0.34 m × 0.35 m with a total vertical height of 1.45 m is considered. The development stages including the ignition, flame-rising and fully-developed fire whirling are modelled successfully through numerical simulations. Fairly good agreements between simulation and experimental results for temperature profiles at the centreline and corner thermocouples are achieved. However, a flame height of 0.3 m to 0.4 m is estimated in the simulation while the experimental observation is around 0.6 m. Also, the temperature is slightly over-predicted at the centre while under-predicted at the corner. These could well be due to the simplified chemistry employed in the FDS. With this preliminary numerical study, it could be logically inferred that the detailed chemical reactions scheme may be needed to capture the fundamental governing characteristics of the fire whirl in future numerical modelling studies.

***Keywords*****:** Fire whirl, Combustion, Large eddy simulation

## 1. Introduction

Fire whirl is a phenomenon in which a fire, under certain air entrainment conditions, acquires vertical vortices and forms a rotating fire along its flame centreline. Owing to the whirling effect, the flame is more centralised at its core hence a whirling fire is normally much thinner and longer than a typical free standing free. Whirling fires occurs frequently in urban and wild land fires, which can cause major damage towards the nature, building and properties, or even threaten human life [1, 2]. For instant, the fire whirl involved in the wildland fire occurred in October, 1871 in Peshitgo, Wisconsin, US, is one of the most serve fire disasters up to date resulting in thousands of fatality and countless amounts of property damages [3]. Nonetheless, over decades of fire research, the complex phenomenon of fire whirl is still not fully clarified and yet to be investigated, mainly due to the lack of quantitative experimental research [4].

Recently, a series of small to medium-scale vertical shaft fire whirl experiments has been carried out by Chow, Zou and co-workers [5-7]. It was demonstrated that the generation of fire whirl could be sub-divided into four stages including (i) initial ignition stage where the flame height is relatively low; (ii) flame rising-up stage where the flame height increase gradually to reach its upcoming state; (iii) stable whirling stage where the flame height is considered to be at its maximum height; (iv) decaying stage where the whirling motion stops and the fire gradually extinguishes.

The objective of this preliminary study is to investigate the fire whirl phenomenon through a numerical standpoint using computational fluid dynamics (CFD) techniques. Numerical simulation assessment is performed based on existing experiment and the following features will be studied and discuss in this paper: (i) the physical behaviour that occurs during the development of a fire whirl; (ii) validation against experimental measurements to ensure the reliability of the adopted methodology; (iii) the flame heights for the flame rising-up and fully developed whirling stages.

## 2. Numerical Model

In this study, the large eddy simulation (LES) based fire field model, namely the Fire Dynamics Simulator (FDS) ver 6.1.2 was utilised. A subgrid-scale (SGS) turbulence model is implemented in FDS along with fully coupled combustion and radiation models to feasibly account for the fire phenomena. It solves numerically a modified form of Navier–Stokes equations appropriate for low-speed flow driven by fire. Second order finite difference scheme is utilised to discretise all spatial derivatives in the conservative equations. Explicit second order predictor– corrector scheme is adopted for updating velocity, pressure, temperature and other essential variables in time.

### 2.1. Governing Equations

Conservation equations of mass, momentum and energy for a Newtonian fluid derived from first principle of physical laws are applied for the fluid motion [8]. The Favre-filtered equations based on density-weighted average of the low-Mach number fluid motion are applied.

$$\frac{\partial \rho}{\partial t} + \nabla(\rho \mathbf{u}) = 0 \tag{1}$$

$$\frac{\partial}{\partial t}(\rho \mathbf{u})\rho + \nabla \cdot (\rho \mathbf{u} \times \mathbf{u} + p\mathbf{I}) = \nabla \cdot \boldsymbol{\tau} + \rho \mathbf{g} \tag{2}$$

$$\frac{\partial}{\partial t}(\rho h)\rho + \nabla \cdot (\rho h \mathbf{u}) = \frac{D\overline{p}}{Dt} + \dot{q}^{"}_{comb} - k\nabla T - \sum_i h_i \rho D_i \nabla Z_i + \dot{q}^{"}_{rad} \tag{3}$$

where $\rho$ is density, $\mathbf{u}$ is the flow velocity, $\nabla$ is the del operator, $\mathbf{I}$ is the identity matrix, $\boldsymbol{\tau}$ is the stress tensor, $\mathbf{g}$ is the gravitational acceleration force. In Eq. 3, $h$ is the enthalpy energy of the flow, $\overline{p}$ is the pressure, $\dot{q}^{"}_{comb}$ is the heat release per unit volume through combustion, the term $-k\nabla T$ and the summation of $\rho h_i D_i \nabla Z_i$ denotes the conductive and diffusive heat fluxes, $\dot{q}^{"}_{rad}$ represents the radiation heat transfer.

### 2.2. Turbulence Model

Since turbulent flow structures contain eddies with a wide range of length and time scales, a special filter is applied in FDS to separate the large and small eddies. The cut-off length of the filter is determined by the simulation grid size. Large eddies are directly resolved while eddies that are smaller than the length scale are predicted by the SGS turbulence model.

### 2.3. Combustion Model

In FDS, the mixture fraction combustion model is adopted, in which mixture fraction is a quantity representing the fuel and products of combustion assuming fuel and oxygen burn instantly when mixed. Unlike the single-step fraction mechanism assuming fuel and oxidizer burn instantaneously when mixed, FDS utilises a two-step reaction scheme to enhance the simulation capability for under-ventilated fire which incorporates an intermediate product CO during its initial step before the final product $CO_2$ is formatted in its second step as illustrated by the following equations:

$$Step\,1: C_x H_y O_z N_a M_b + v_{O_2} O_2 \rightarrow v_{H_2O} H_2O + v_{CO} CO + v_{soot} soot + v_{N_2} N_2 + v_M M \tag{4}$$

$$Step\,2: v_{CO}\left(CO + \frac{1}{2} O_2\right) \rightarrow v_{CO} CO_2 \tag{5}$$

## 3. Experimental Configuration and Numerical Setup

A series of tests were carried out by Chow and Han [7] in a small-scale vertical shaft model as illustrated in Fig. 1. The base of the model was 0.34 m × 0.35 m and the vertical height is 1.45 m. It should be noted that the top of the model was opened to the surroundings. During the experiment, four tests were conducted separately with four different sizes of circular ethanol pool fuel beds placed at the centre of the model (i.e. pool areas of 21, 26, 33 and 39 $cm^2$ respectively). A vertical gap with a width size of 0.036 was placed at one side of the 0.34 m wall to allow the generation of the fire whirl effect as illustrated in Fig. 1a. In order to indicate the location of the flame and to measure the hot plume temperature during the fire whirling process, two sets of vertical thermocouples were positioned at the centre and corner of the vertical shaft as depicted in Fig. 1b respectively by THCP and THCR.

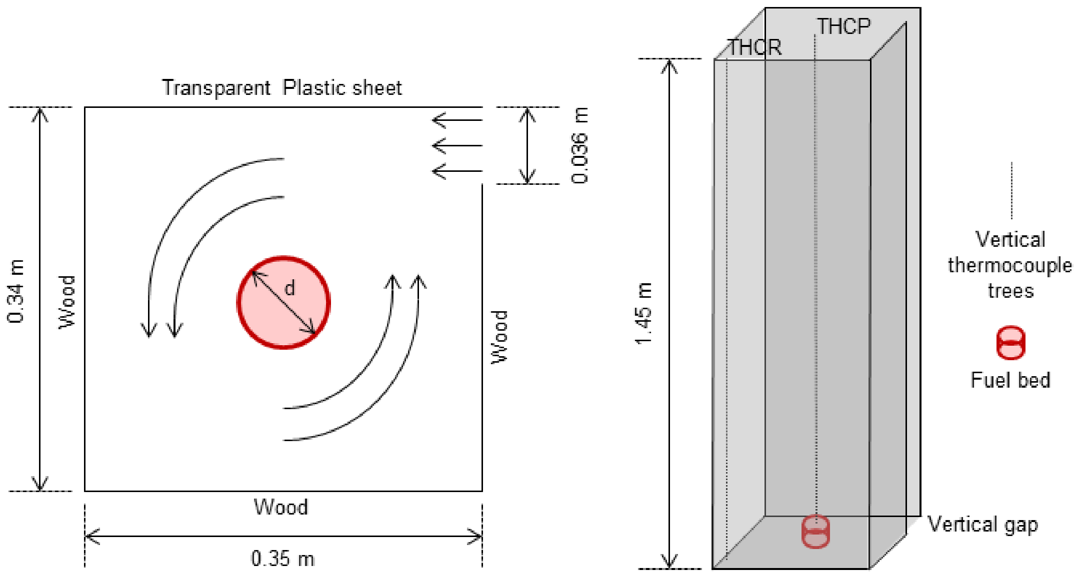


(a) (b)

Fig. 1: Schematic sketch of (a) top view and (b) three-dimensional view of the vertical shaft fire whirl model.

### 3.1. Modelling Configuration and Boundary Conditions

The computational domain is extended 0.15 m in x-direction and 0.05 m in y-direction to allow the flow across the vertical gap to be aptly modelled. Therefore, the size of the domain including the extended region is 0.5 m × 0.4 m × 1.45 m. For the purpose of maintaining numerical stability, an equally spaced mesh system is applied where each segment is 0.05 m × 0.05 m × 0.05 m, adding together a total amount of 2,320,000 grid cells. This choice of grid size satisfies the requirement as stipulated in FDS guidelines for the non-dimensional characteristic length analysis [8]. In order to validate the simulation, four simulation cases with different heat release rates are considered numerically as summarised in Table 1.

Table 1: Fuel bed boundary condition for numerical simulation cases 1 - 4.

| | Experiment Fuel Pan no. | Pool size, $m^2$ | Measured heat release rate, kW |
|---|---|---|---|
| Case 1 | P1 | 39 | 3.58 |
| Case 2 | P2 | 33 | 3.30 |
| Case 3 | P3 | 26 | 2.36 |
| Case 4 | P4 | 21 | 2.25 |

## 4. Results and Discussions

Since in the experiment the four tests were carried out for around 500 s to 600 s, the total simulation time was prescribed as 600 s in the simulation. It should be noted that steady-state temperature results were measured in the experiment. For the purpose of comparisons, time-average was applied to obtain the numerical temperature predictions. It was found that generally for all four cases the fire whirl is fully developed after a total simulation time of 50 s. Hence, the results were obtained through time-average of numerical data from 100 s to 600 s. Additional thermocouples are placed near the flame region to capture the temperature at the flaming region (i.e. 0.01 m vertical height spacing in between from 0.02 m to 0.1 m). Afterwards, the vertical distance between each thermocouple is 0.1 m from 0.1 m to 3.58 m.

### 4.1. Temperature Comparisons

Fig. 2 shows the centreline thermocouple experimental measurements against numerical predictions for different fire sizes. As can be seen, the overall numerical temperature profiles for all four heat release rates were in reasonable agreement with the experimental data. The temperature near the flaming region (i.e. below 0.4 m) is accurately predicted especially for large fire sizes (i.e. 3.58 kW and 3.30 kW). It should be addresses that the flame core (i.e. maximum temperature point) is located at around 0.02 to 0.03 m vertical height in general, which is just slightly above the fuel bed. This means that the fuel (i.e. ethanol vapour) and oxygen are mixed instantaneously partially accelerated by the whirling effect. Nevertheless, the temperature upon the flaming region is over-predicted for all simulation cases. This could be due to the following reasons. Firstly, in the experiment the materials used for the walls of the vertical shaft were wood and plastic sheet, which might have a significant amount of heat lost to the surroundings. During the simulation, the walls were considered as adiabatic hence the heat energy aggregate within the vertical shaft is considerably higher. Secondly, the simplified chemistry applied for the combustion model in FDS might over-predict the amount of heat generated since the combustion process is almost 100 % efficient.

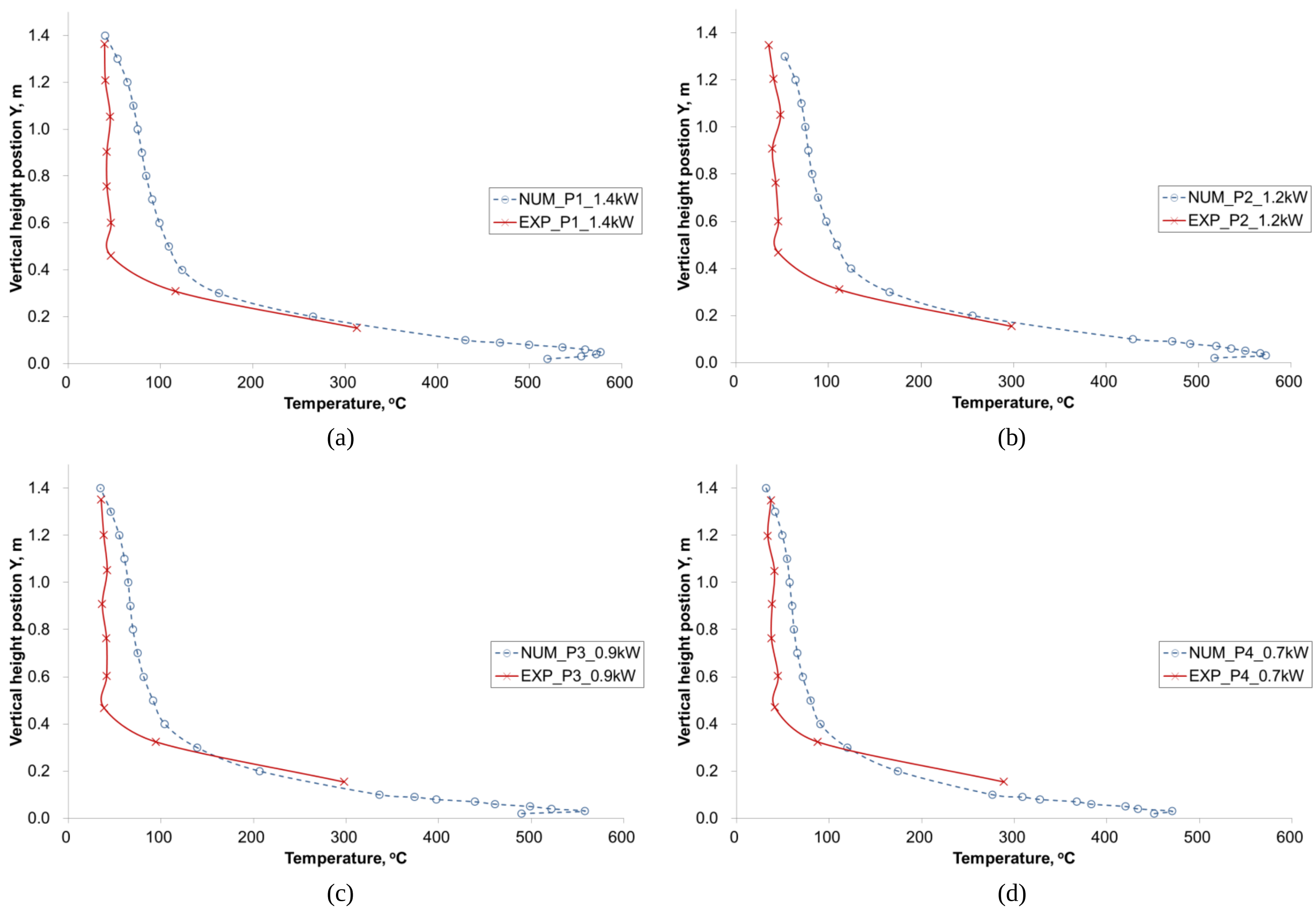


Fig. 2: Centreline temperature comparisons between numerical and experiment for (a) 3.58 kW, (b) 3.30 kW, (c) 2.36 kW and (d) 2.25 kW fire.

As for the temperature at the corner, it is observed that the temperature gets higher along the vertical height, which the trend is also captured in the numerical model as illustrated in Fig. 3. It should be noted that the experimental results reported could be averaged values of instantaneous records over a short but unmentioned window of time. With the fire whirl concentrated around the centre axis, the experimental temperatures measurements exhibited a rising trend with height but not monotonic. Nevertheless, overall speaking, the temperature profiles are fairly reasonably predicted at the corner although under-predictions of around 5 $^{o}$C are observed. Owing to the fact that more heat is generated at the centre of the vertical shaft as demonstrated in Fig. 2, it is speculated that the heat diffusivity in FDS is slightly lower than that in reality. Hence the temperature estimated at the near fire region is higher while other region is consequently lower.

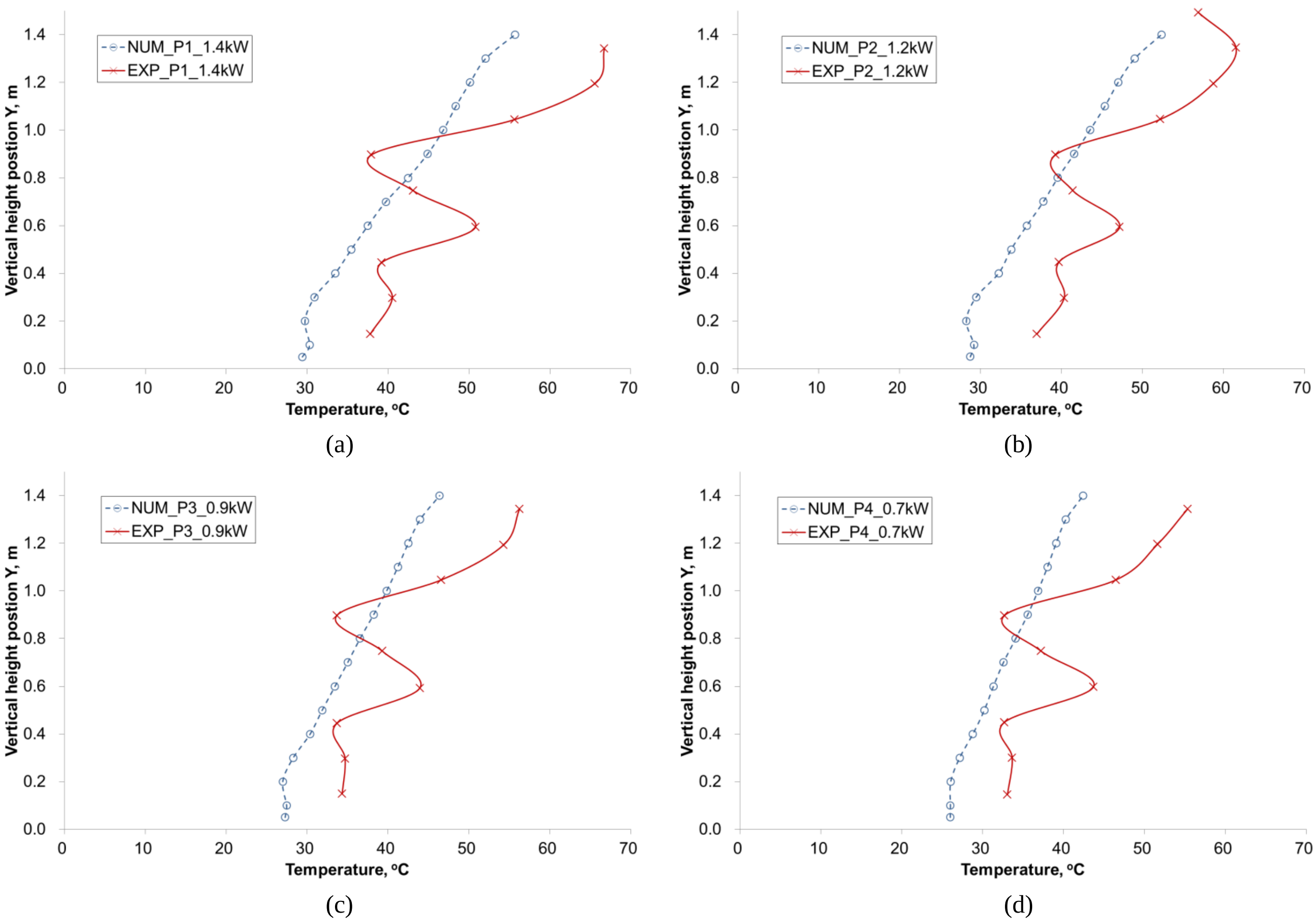


Fig. 3: Corner thermocouple tree temperature comparisons between numerical and experiment for (a) 3.58 kW, (b) 3.30 kW, (c) 2.36 kW and (d) 2.25 kW fire.

### 4.2. Flame and Hot Plume Development

The temperature contours cutting at the centre of the fuel bed (i.e. 0.17 m in y-direction) for various time instants are shown in Fig. 4. Provided that visible flame in red colour is around 525 $^{o}$C in temperature and the flame tips in yellow (i.e. barely visible by human naked eye) is around 350 $^{o}$C [9], the range of the contour is set as 20 $^{o}$C to 525 $^{o}$C for the ease to indicate the fire and the corresponding hot plume generated. As a result, the yellow scale for the contour plot now represents the minimum temperature that can be visualised as a flame. After the fire whirl is fully developed, the numerical prediction for the height of the flame by observation was around 0.3 m to 0.4 m. The capture footage in the experiment as depicted in Fig. 5 suggests that the actual flame height was around 0.6 m tall, provided that in the experiment each thermocouples were separated by 0.15 m and the flame reached the height of the forth thermocouple (i.e. 0.6 m). As shown in Fig. 4 (h) at 400s, the developed fire whirl in numerical simulation compares well with the experimental image in Fig. 5

qualitatively. The difference in flame height could be due to nature of mixture fraction based combustion model implemented in FDS. Since the model is based on the assumption of mixed-is-burnt, meaning that combustion occurs directly when fuel mixes with oxygen, most of the combustion process happens near the fuel bed. In reality, the combustion is never 100 % complete and intermediate chemical species forms during the process [10-12].

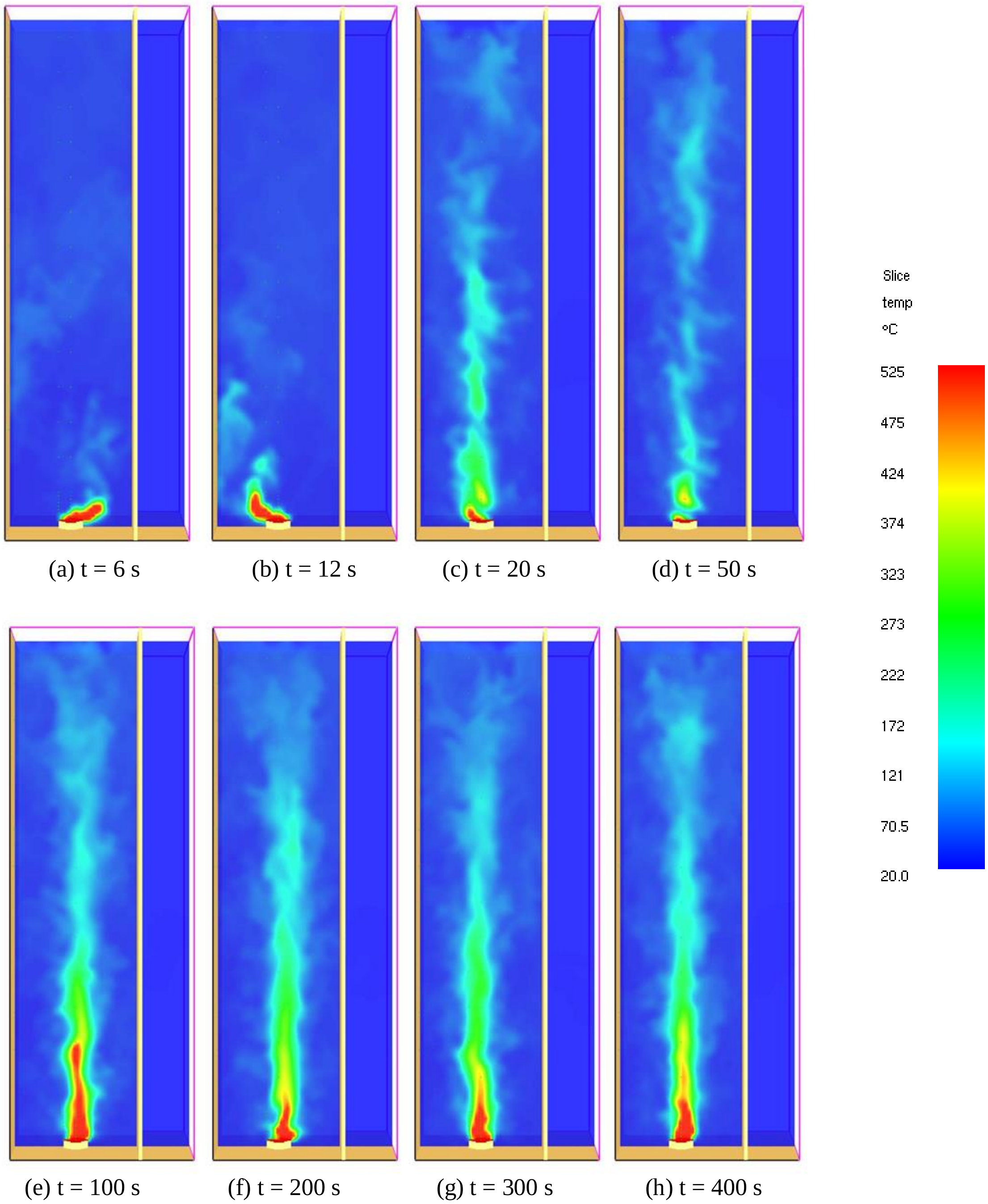

Fig. 4: Temperature contours cutting at fuel bed centre (i.e. y = 0.17 m) for various time instants showing fire whirl developing stage (a) – (d) and the fully developed stage (e) – (h) for simulation Case 1.

### 4.3. Centre-core for the Fire Whirl

During the development stage of the fire whirl, the centre-core of the flame spins around the centre of the fuel bed. In Fig. 6, the velocity vector results at height level of 0.1 m gives an indication of the location of the flame core. Initially, air is entrained by the fire through the vertical gap. As this incoming flow is gradually established, if forms a rotational force within the vertical causing the fire whirl. As indicated, during the period of from 0 s to 50 s before the fire whirl is fully developed, the centre-core of the flame rotates around the centreline of the fuel bed. Hence, the fire leans towards the walls of the vertical shaft and became flat in terms of vertical height as can be demonstrated by the temperature contours in Fig 4a – c.

Fig. 5: Experimental footage of the fire whirl for 3.58 kW ethanol fire after Chow and Han [7].

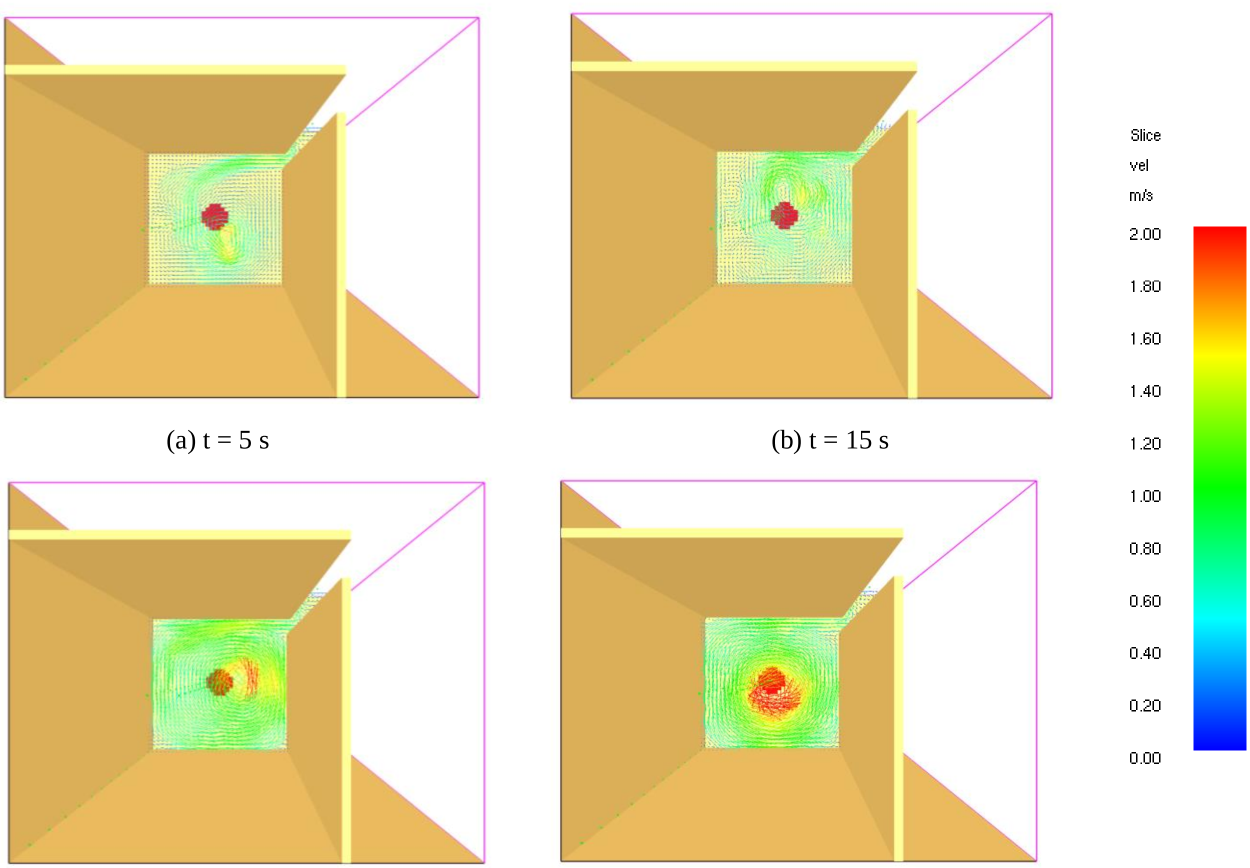


(a) t = 5 s (b) t = 15 s

(c) t = 25 s (d) t = 45 s

Fig. 6: Velocity vector plots cutting at vertical plane (z = 0.1 m) at various time instants for simulation Case 1.

## 5. Conclusion

In this article, the fire whirl phenomenon of a small-scale ethanol pool fire in a vertical shaft with one vertical gap was investigated numerically. Large eddy simulation was applied along with a mixture fraction based combustion model to simulate the temporal rotating flame core and macroscopic fuel air mixing behaviour. The key findings includes: (i) during fire whirl initial stage, the flame leans towards the wall and the flame height is relatively shorter; (ii) once the fire whirl was fully developed, the flame rotational core centres at the fuel bed centreline and the flame height significantly increases. (iii) the flame height for a fully-developed fire are 3 m to 4 m for numerical and 6 m for the experiment; (iv) overall temperature profiles are in reasonably well agreement with experiment with a slight over-prediction at the centreline and under-prediction at the corner respectively. This preliminary numerical study demonstrated that the detailed chemical reactions scheme may be needed in future numerical modelling studies to better describe the fundamental governing characteristics of the fire whirl.

## Acknowledgements

The paper is sponsored by the Australian Research Council (ARC Linkage Project LP140100121). All financial and technical supports are deeply appreciated by the authors.

## References

[1] K. Kuwana, K. Sekimoto, K. Saito, and F. A. Williams, "Scaling fire whirls," *Fire Safety Journal*, vol. 43, pp. 252-257, 2008.

[2] S. Soma and K. Saito, "Reconstruction of fire whirls using scale models," *Combustion and Flame*, vol. 86, pp. 269-284, 1991.

[3] P. Jimeo. (1871, October 8). History of the Peshtigo fire [Online]. Available: http://www.wisconsinhistory.org.

[4] J. Lei, N. Liu, L. Zhang, H. Chen, L. Shu, P. Chen, *et al.*, "Experimental research on combustion dynamics of medium-scale fire whirl," *Proceedings of the Combustion Institute*, vol. 33, pp. 2407-2415, 2011.

[5] W. K. Chow, Z. He, and Y. Gao, "Internal Fire Whirls in a Vertical Shaft," *Journal of Fire Sciences*, vol. 29, pp. 71-92, 2011.

[6] G. W. Zou and W. K. Chow, "Generation of an internal fire whirl in an open roof vertical shaft model with a single corner gap," *Journal of Fire Sciences*, 2015.

[7] W. K. Chow and S. S. Han, "Experimental data on scale modelling studies on internal fire whirls," *International Journal on Engineering Performance-Based Fire Codes*, vol. 10, pp. 63-74, 2011.

[8] K. McGrattan, S. Hostikka, R. Mcdermott, J. Floyd, C. Weinschenk, and K. Overholt, "Fire Dynamics Simulator (FDS Version 6.0.1) Technical Reference Guide, vol. 1 Mathematical model," National Institute of Standards and Technology, 2013.

[9] S. C. P. Cheung and G. H. Yeoh, "A fully-coupled simulation of vortical structures in a large-scale buoyant pool fire," *International Journal of Thermal Sciences*, vol. 48, pp. 2187-2202, 2009.

[10] A. C. Y. Yuen, G. H. Yeoh, V. Timchenko, S. C. P. Cheung, and T. J. Barber, "Importance of detailed chemical kinetics on combustion and soot modelling of ventilated and under-ventilated fires in compartment," *International Journal of Heat and Mass Transfer*, vol. 96, pp. 171-188, 2016.

[11] A. C. Y. Yuen, G. H. Yeoh, V. Timchenko and T. J. Barber, "LES and multi-step chemistry reaction in compartment fires," *Numerical Heat Transfer, Part A*, vol. 68, pp. 711-736, 2015.

[12] A. C. Y. Yuen, G. H. Yeoh, V. Timchenko, S. C. P. Cheung, and T. J. Barber, "Study of three LES subgrid-scale turbulence models for predictions of heat and mass transfer in large-scale compartment fires," *Numerical Heat Transfer*, 2016.